Journal of Structural Geology, Vol. 11, No. 8, pp. 1045 to 1049, 1989
Printed in Great Britain

0191-8141/89 $03.00+0.00

Brevia

SHORT NOTE

Toward a unified conceptual framework for shear-sense indicators

M. Bjornerud

Geology Department, Miami University, Oxford, OH 45056, U.S.A.

(*Received* 16 *February* 1989; *accepted in revised form* 10 *July* 1989)

Abstract—The growing lexicon for shear-sense indicators has created a need for a unified conceptual system of classification. Many common shear structures can be described by linear combinations of two kinematic variables which quantify the relative importance of objects vs foliations in controlling the shear-zone velocity field.

INTRODUCTION

Structural geologists command a growing repertoire of practical criteria for inferring shear sense in rock (see, for example, *J. Struct. Geol.*, Vol. 9, No. 5/6, 1987). The nomenclature for these shear-sense indicators has become increasingly elaborate as new types of structures are recognized. The purpose of this paper is to suggest a two-variable kinematic scheme for classifying some common shear-generated meso- and microstructures. Such a scheme may help to (1) clarify the kinematic relationships among currently used shear-sense indicators and (2) eliminate the need for neologies as new variations are identified.

ISOLATING APPROPRIATE SHEAR-ZONE DESCRIPTORS

Identifying variables for a shear-zone classification system is not trivial. The variables should be able to describe the widest possible range of shear-zone features. The ideal variables would be 'basis vectors' which span the vector space of all shear-zone structures, enabling some linear combination of the variables to characterize any shear zone. Several important studies have related the development of certain shear-zone features to finite shear strain (e.g. Hudleston 1980, White *et al.* 1980, Wilson 1984) or to various geometrical and mechanical characteristics such as porphyroclast shape, orientation and recrystallization rate (Passchier & Simpson 1986, Passchier 1987). It may be useful, however, to isolate kinematic variables which encompass these types of parameters, such that the physical characteristics of a given shear zone at a given time could be represented by particular values of these higher-order variables.

From a kinematic perspective, the morphologies of shear-generated structures can be considered records of spatial variations in strain rate within a shear zone. Characterization of strain-rate gradients is therefore a potential basis for a shear-zone classification scheme. As a starting point for such a scheme, shear-sense indicators might be classed according to the relative kinematic importance of objects vs foliations in their development. The form of object-dominated indicators (e.g. porphyroclast systems) is controlled by the shear-induced rotation of objects in the shear zone, while the form of foliation-dominated indicators (e.g. *S–C* fabrics) is controlled by the relative slip rates along surfaces in the shear zone. This dichotomy is explored below.

Quantifying object dominance

A possible measure of object dominance is the degree of coupling between an object and its shearing matrix, as measured by the spatial velocity gradient at the object–matrix boundary in the direction perpendicular to the boundary (Fig. 1). In a polar co-ordinate system centered on an object of circular cross-section and unit radius, the object–matrix boundary velocity gradient would be dv/dr at $r=1$ (where v is the position-dependent particle velocity and r is the radial distance from the object center). If an object is absolutely rigid relative to the shearing matrix, the shear-induced vorticity of the matrix is converted at the object boundary into spin vorticity within the object (rotation relative to an external reference frame) (Lister & Williams 1983). If there is no velocity gradient across the object–matrix boundary (i.e. a no-slip boundary, Fig. 1a), the angular velocity of the object will equal half the bulk shear rate (Jeffrey 1922, Freeman 1985). As it rotates, the object will pull adjacent parts of the matrix with it. If the matrix is layered, asymmetric folds will develop next to the object (Simpson & Schmid 1983).

If, in contrast, there is a velocity gradient across the

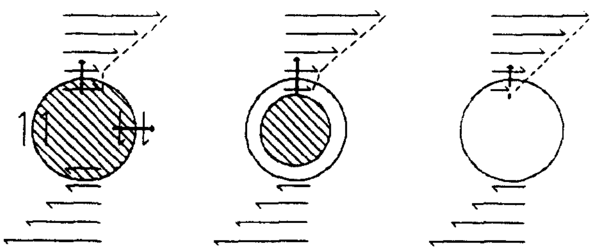

Fig. 1. Object–matrix boundary velocity gradient, a measure of object-dominance. In each part, thin arrows represent local velocity vectors, dark arrow shows direction in which gradient is measured, and broken line shows shear rate. (a) Low object–matrix boundary gradient (no-slip boundary). Object (shaded) is perfectly rigid relative to matrix. (b) Moderate object–matrix boundary gradient (slipping boundary). Slip may be accomplished by deformation of outer part of the object, as illustrated, or by dissolution and reprecipitation of matrix material at the object–matrix contact. (c) High object–matrix boundary gradient. Illustrated is the limiting case in which the object is completely passive and the object–matrix boundary velocity gradient is equal to the overall shear rate.

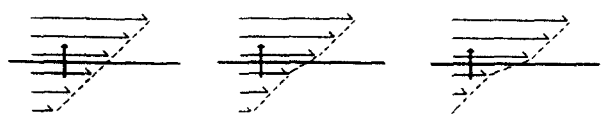

Fig. 2. Transverse shear-rate gradient, a measure of foliation dominance. In each part, thin arrows represent local velocity vectors, dark arrow shows direction in which gradient is measured, and broken line shows shear rate. (a) Low transverse shear-rate gradient (homogeneous simple shear; passive foliation). (b) Moderate transverse shear-rate gradient. (c) High transverse shear-rate gradient.

object–matrix boundary (i.e. a slipping boundary, Fig. 1b), the shear-vorticity–spin-vorticity transition will occur across a zone rather than a sharp surface. Pure spin may be important only in the core of the object. The object will thus be partly decoupled from the shearing matrix and will not strongly influence flow in the matrix. In natural shear zones, such decoupling may arise from deformation and recrystallization of the object (porphyroclast tails) or dissolution and reprecipitation of matrix material (pressure shadows). In the limiting case, no part of the object spins, and the entire object deforms passively with the matrix. For this case, the object–matrix boundary velocity gradient has its maximum possible value: the shear rate of the surrounding matrix (Fig. 1c). In summary, object-dominated shear zones can be characterized by object–matrix boundaries with low velocity gradients and sharp vorticity partitioning. Conversely, shear zones with low object dominance reflect finite velocity gradients and diffuse vorticity partitioning across object–matrix boundaries.

Quantifying foliation dominance

An analogous kinematic descriptor of foliation dominance is the spatial gradient in shear-strain rate across shear planes in a shear zone (Fig. 2). If the shear direction is parallel to the x axis of a Cartesian co-ordinate system, the transverse shear-rate gradient is $d/dy\ (d\gamma/dt)$ at the y co-ordinate of a particular shear plane (where γ is the time- and position-dependent shear strain). This gradient is zero at every point in a zone of homogeneous simple shear because there is no change in the rate of shear strain across the zone (Fig. 2a). The transverse shear-rate gradient is non-zero, however, if the shear rate along certain material planes is higher than the shear rate elsewhere in the shear zone (Figs. 2b & c). The planes of relatively rapid shear will then act as the dominant components in the system, controlling the kinematic response of material between them. (The kinematic dominance of particular shear planes also depends on the relative spacing of these slipping planes.) In summary, high transverse shear-rate gradients correspond to high foliation dominance (active behavior) while low gradients correspond to low foliation dominance (passive behavior).

LINEAR COMBINATIONS OF THE VARIABLES

How well do these two shear zone descriptors—object–matrix boundary velocity gradient and transverse shear-rate gradient—span the space of possible shear-zone features? How do these kinematic variables correspond to 'real' shear-zone variables? Figure 3 shows nine categories of shear structures corresponding to linear combinations of low, intermediate and high values of the two kinematic variables. Each of these categories will be examined briefly. The order in which the categories are discussed is not meant to connote temporal evolution, but to illustrate how common shear-sense indicators can be represented within a two-dimensional kinematic continuum.

Category a: *Low object–matrix boundary velocity gradient, low transverse shear-rate gradient*

This is the most purely object-dominated category of shear structures. There is no differential movement between the object and its passive matrix. Induced to rotate by the shearing matrix, the object itself influences the local flow field in the matrix by pulling matrix material with it along its no-slip boundary. In a layered medium, asymmetric microfolds develop next to the object and provide unambiguous shear-sense information (Simpson & Schmid 1983, fig. 4G). The rotating object will also perturb the simple shear velocity field in the passive matrix up to several radii from the object center (Langlois 1964). If layer spacing is on the order of the object radius, asymmetric folds will develop on the downshear sides of the object as layers are rotated into positions oblique to the shear direction (Hudleston 1976). Such folds have been simulated mathematically (Bjornerud 1989) and generated in silicon scale models by Van den Driessche & Brun (1987), who called them "rolling structures". If the matrix is not layered or if layer spacing is large relative to the object diameter, the object-induced deformation of the matrix may not be

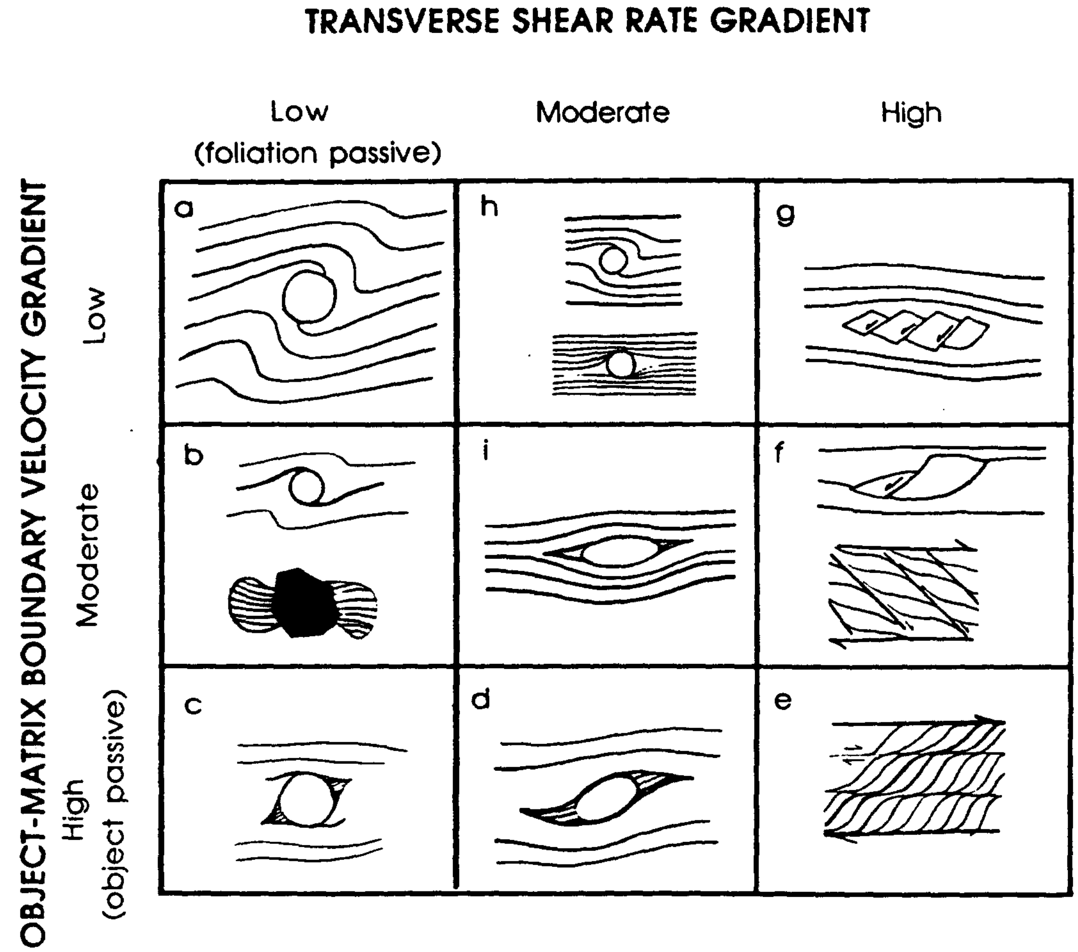

Fig. 3. Linear combinations of the two kinematic variables. Object-dominated shear structures appear in top row; foliation-dominated structures in right column. (a) Rolling structures (Van den Driessche & Brun 1987, Bjornerud 1989). (b) δ-type porphyroclasts (Passchier & Simpson 1986) and asymmetric pressure shadows (Durney & Ramsay 1973). (c) Hybrid δ–σ porphyroclasts (Passchier & Simpson 1986). (d) σ-type porphyroclasts (Passchier & Simpson 1986). (e) Type I *S–C* fabrics (Berthé *et al.* 1979, Lister & Snoke 1984). (f) Type II *S–C* fabrics (Lister & Snoke 1984) and extensional crenulation cleavage, shear bands, etc. (Platt & Vissers 1980, Dennis & Secor 1987). (g) Fractured grains and clasts (Simpson & Schmid 1983). (h) Damped rolling structures and θ porphyroclasts. (i) Ambiguous (symmetrical) structures.

visible and no useful shear-sense information will be recorded.

Category b: *Moderate object–matrix boundary velocity gradient, low transverse shear-rate gradient*

In this category, there is some decoupling between object and matrix and thus the influence of object rotation on matrix flow is diminished. Matrix layering, if it exists, is still mechanically passive. Asymmetric microfolds will develop in layers adjacent to the object, but the fold amplitude at a given shear strain will not be as great as for no-slip boundaries. If layer spacing is small relative to object size, folds may develop further out in the matrix, but they will not propagate as far as in a tightly coupled object–matrix system. Natural shear-sense indicators in this category include asymmetric pressure shadows around resistant objects (Durney & Ramsay 1973, Etchecopar & Malavieille 1987) and δ-type porphyroclasts (Passchier & Simpson 1986). In the case of pyrite-type pressure shadows (Ramsay & Huber 1983, pp. 265–269), differential object–matrix movement is expressed as pressure solution of matrix material at points of stress concentration on the object–matrix contact. For crinoid-type pressure shadows, object material is dissolved and reprecipitated. For δ-porphyroclasts, object–matrix slip is allowed by recrystallization of the outer part of the porphyroclast. Passchier & Simpson (1986), who systematized the analysis of shear-zone porphyroclasts, suggested that δ-porphyroclasts develop when the ratio of shear rate to recrystallization rate is relatively high. From a kinematic perspective, the recrystallization rate represents the velocity gradient across the object–matrix boundary.

Categories c *and* d: *High object–matrix boundary velocity gradient, low to moderate transverse shear-rate gradient*

In these categories, slip at the object–matrix contact is significant, and the shear-vorticity–spin-vorticity transition occurs over a broad zone. As a result, features related to object rotation are subdued or absent.

If the matrix is also passive (no transverse shear rate gradient; category *c*), neither the object nor the foliation is kinematically dominant. The result may be mixed δ–σ porphyroclast systems (Passchier & Simpson 1986) exhibiting both (1) minor δ-type microfolds of material pulled with the object, and (2) small recrystallized σ-type tails dragged into the overall shear direction. Passchier & Simpson (1986) suggest, however, that mixed δ–σ porphyroclasts may require an increase in shear-strain rate over time. Such time dependence of strain rate is not represented in the two-dimensional continuum of Fig. 3.

If the matrix is not completely passive (finite transverse shear-rate gradient; category *d*), true σ porphyroclasts will be produced because the magnitude of the velocity-field perturbation produced by the object will be smaller than the relatively rapid shear rate on certain material planes.

Category e: *High object–matrix boundary gradient, high transverse shear-rate gradient*

This is the most purely foliation-dominated category of shear structures. A single family of slip planes dictates the kinematic behavior of the zone. Objects, if present, exert no control on the velocity field in the matrix, but passively record the state of cumulative strain in the regions between the planes of easy slip. The obvious geologic expression of this category is the Type I *S–C* fabric (Berthé *et al.* 1979, Lister & Snoke 1984), in which slip is concentrated along *C* (shear) surfaces while *S* (finite flattening) surfaces develop in the material in between. Passchier & Simpson (1986) illustrated the morphologic link between σ porphyroclasts and *S–C* fabrics. I suggest that the only kinematic difference between these two end-member structures is the relative magnitude of shear-rate gradients across their respective shear planes.

Category f: *Moderate object–matrix boundary gradient, high transverse shear-rate gradient*

In this category, rapidly slipping shear planes are again kinematically dominant, but the intervening material is not totally passive. Instead, shear-vorticity–spin-vorticity partitioning occurs within subdomains between the planes. Type II *S–C* fabrics in which mica porphyroblasts spawn mica 'fish' (Lister & Snoke 1984) are one geologic expression of this category. The mica porphyroblasts have some finite strength relative to the surrounding material between the shear planes, and they convert the shear-induced vorticity of this material to spin vorticity by spalling off the 'fish' which rotate with respect to an external reference frame.

Other examples of category *f* structures are extensional crenulation cleavages (Platt & Vissers 1980), shear bands (White *et al.* 1980) and *P*-shears (Tchalenko 1970). Dennis & Secor (1987) and Mawer & White (1987) have suggested that these features share the same kinematic function. In each case, subdomains between shear planes undergo rotation relative to an external reference frame, in addition to some deformation. Dennis & Secor (1987) have shown that these rotations collectively act to maintain the orientation of the shear zone by effecting net displacement in the overall slip direction. This is consistent with the idea that the high transverse shear-rate gradient across the shear planes is dominant over object–matrix vorticity partitioning between these planes.

Category g: *Low object–matrix boundary gradient, high transverse shear-rate gradient*

In this category, mechanically active objects and foliations compete for kinematic dominance. As in the previous two categories, shear planes are well-defined; but so too are object–matrix boundaries. Shear-vorticity–spin-vorticity partitioning occurs at a sharp surface. A geologic example is a grain or clast that has fractured but undergone no plastic deformation in a mylonite. The rotation of such an object may have been inhibited by its inequant shape and its orientation relative to the rapidly slipping planes (Passchier 1987), but its rigidity relative to the shearing matrix necessitated some type of vorticity conversion. Slip along oblique surfaces accomplished the conversion to spin vorticity. The orientation of these secondary slip planes may not provide reliable shear-sense information, as they may have been pre-existing surfaces along which rotation was most easily accommodated (Dennis & Secor 1987).

Category h: *Low object–matrix boundary gradient, moderate transverse shear-rate gradient*

This category is object-dominated, but shear-rate gradients across shear planes are significant enough to partly counteract the object's kinematic control of the matrix. The object rotates and pulls adjacent matrix material with it. In a layered matrix, asymmetric folds develop next to and outward from the object as in category *a*, but the folds are not likely to propagate across shear planes, because the transverse shear-rate gradient will be greater than the object-induced velocity perturbation in the far field. The resultant structures might be called "damped rolling structures", as the moderately active shear planes act to subdue the kinematic effect of the object. These structures are distinct from δ porphyroclasts in that the material which forms the visible spiral around the object is matrix layering, rather than a recrystallized mantle derived from the porphyroclast.

Other structures which could be classed in this category are θ porphyroclasts (Hooper & Hatcher 1988). The morphology of θ-type systems is rather puzzling, however. Although the porphyroclasts lack recrystallized mantles (indicating little decoupling of object and matrix), the perturbation of layering around the porphyroclasts does not seem commensurate with the finite shear strains that the host mylonites appear to record. This may indicate that θ porphyroclasts, like mixed δ–σ porphyroclasts, reflect a temporal change in strain-rate gradients within the shear zone, in which an initially passive matrix becomes increasingly foliated and kinematically dominant as deformation progresses.

Category i: *Moderate object–matrix boundary gradient, moderate transverse shear-rate gradient*

Both objects and foliations exert kinematic control in this category. The object is slightly decoupled from the matrix, and the effects of object rotation are counterbalanced by the effects of relatively rapid slip on shear planes. Geologic structures in this category are frustratingly common: porphyroclasts, pressure shadows, and deformed grains which are symmetrical with respect to the mylonitic foliation and yield no clear shear-sense information.

CONCLUSIONS

Common shear-sense indicators with a wide range of morphologies can be portrayed within a two-dimensional kinematic continuum according to the relative importance of objects vs foliations in controlling flow within the shear zone. Object dominance, measured by the velocity gradient at an object–matrix boundary in the direction orthogonal to that boundary, is a function of interrelated variables including: (1) compositional and mechanical contrasts between the object and matrix; (2) the object shape and orientation relative to the shear planes; and (3) deformation and recovery mechanisms and rates (e.g. extent of pressure solution of the matrix next to a pyrite crystal, or the rate of recrystallization of a porphyroclast mantle). Foliation dominance, expressed by the shear rate gradient across planes subparallel to the shear zone, is dependent on natural variables such as: (1) the existence and mechanical properties of pre-deformation layering; (2) deformation mechanisms and metamorphic differentiation; and (3) finite strain and strain history of the shear zone (and associated grain-size reduction or development of dimensional- and lattice-preferred orientation) (White *et al.* 1980, Burg *et al.* 1986).

The objective of this paper has been to illustrate the kinematic unity of seemingly distinct species of shear-sense indicators. It is likely, however, that the 'vector space' of shear-zone features is not two-dimensional but three- or poly-dimensional. Additional variables may be necessary to describe other types of shear-generated structures. In particular, temporal changes in strain-rate gradients, related to changing frictional behavior or to heterogeneous volume loss, almost certainly influence the morphologies of some shear-zone structures. In addition, most natural structures probably develop under some combination of progressive simple and progressive pure shear, so strain-rate gradients in the third dimension must also be considered. The present classification scheme therefore represents only one planar projection of the kinematic vector space of shear-generated features.

Acknowledgements—I wich to thank A. J. Dennis, R. Hatcher, C. Teyssier and R. Gower for thoughtful reviews and comments.

REFERENCES

Berthé, D., Choukroune, P. & Jegouzo, P. 1979. Orthogneiss, mylonite and non-coaxial deformation of granites: the example of the South Armorican shear zone. *J. Struct. Geol.* **1**, 31–42.
Bjornerud, M. 1989. Mathematical model for folding of layering near rigid objects in shear deformation. *J. Struct. Geol.* **11**, 245–254.
Burg, J.-P., Wilson, C. & Mitchell, J. 1986. Dynamic recrystallization and fabric development during the simple shear deformation of ice. *J. Struct. Geol.* **8**, 857–870.
Dennis, A. & Secor, D. 1987. A model for the development of crenulations in shear zones with applications from the Southern Appalachian Piedmont. *J. Struct. Geol.* **9**, 809–817.
Durney, D. & Ramsay, J. 1973. Incremental strain measured by syntectonic crystal growths. In: *Gravity and Tectonics* (edited by DeJong, J. & Scholten, R.). John Wiley, New York, 67–96.
Etchecopar, A. & Malavieille, J. 1987. Computer models of pressure shadows: a method for strain measurement and shear-sense determination. *J. Struct. Geol.* **9**, 667–678.
Freeman, B. 1985. The motion of rigid particles in slow flows. *Tectonophysics* **34**, 163–183.
Hooper, R. & Hatcher, R. 1988. Mylonites from the Towaliga fault zone, central Georgia: products of heterogeneous non-coaxial deformation. *Tectonophysics* **152**, 1–17.
Hudleston, P. 1976. Recumbent folding in the base of the Barnes ice cap, Baffin Island, NW Territories, Canada. *Bull. geol. Soc. Am.* **87**, 1684–1692.
Hudleston, P. 1980. The progressive development of inhomogeneous shear and crystallographic fabric in glacial ice. *J. Struct. Geol.* **2**, 189–196.
Jeffrey, G. 1922. The motion of ellipsoidal particles immersed in a viscous fluid. *Proc. R. Soc. Lond.* **A102**, 161–179.
Langlois, W. 1964. *Slow Viscous Flow*. Macmillan, New York.
Lister, G. & Snoke, A. 1984. S–C mylonites. *J. Struct. Geol.* **6**, 617–638.
Lister, G. & Williams, P. 1983. The partitioning of deformation in flowing rock masses. *Tectonophysics* **92**, 1–33.
Mawer, C. & White, J. 1987. Sense of displacement on the Cobequid–Chedabucto fault system, Nova Scotia, Canada. *Can. J. Earth Sci.* **24**, 217–223.
Passchier, C. 1987. Stable position of rigid objects in non-coaxial flow—a study in vorticity analysis. *J. Struct. Geol.* **9**, 679–690.
Passchier, C. & Simpson, C. 1986. Porphyroclast systems as kinematic indicators. *J. Struct. Geol.* **8**, 831–843.
Platt, J. & Vissers, R. 1980. Extensional structures in anisotropic rocks. *J. Struct. Geol.* **2**, 397–410.
Ramsay, J. & Huber, M. 1983. *The Techniques of Modern Structural Geology. Vol. 1: Strain Analysis*. Academic Press, New York.
Simpson, C. & Schmid, S. 1983. An evaluation of criteria to deduce sense of movement in sheared rocks. *Bull. geol. Soc. Am.* **94**, 1281–1288.
Tchalenko, J. 1970. Similarities between shear zones of different magnitudes. *Bull. geol. Soc. Am.* **81**, 1625–1640.
Van den Driessche, J. & Brun, J.-P. 1987. Rolling structures at large shear strain. *J. Struct. Geol.* **9** 691–704.
White, S., Burrows, S., Carreras, J., Shaw, N. & Humphreys, F. 1980. On mylonites in ductile shear zones. *J. Struct. Geol.* **2**, 175–187.
Wilson, C. 1984. Shear bands, crenulations and differentiated layering in ice–mica models. *J. Struct. Geol.* **6**, 303–319.